DIRECTION OF ARRIVAL ESTIMATION OF HUMANS WITH A SMALL SENSOR ARRAY USING AN ARTIFICIAL NEURAL NETWORK

Y. Kim

Department of Electrical and Computer Engineering
California State University at Fresno, USA

H. Ling

Department of Electrical and Computer Engineering
University of Texas at Austin, USA

Abstract—An array processing algorithm based on artificial neural networks (ANNs) is proposed to estimate the directions of arrival (DOAs) of moving humans using a small sensor array. In the approach, software beamforming is first performed on the received signals from the sensor elements to form a number of overlapping beams. The received signals from all the beams produce a unique "signature" in accordance with the target locations as well as the number of targets. The target tracking procedure is handled by two separate ANNs in sequence. The first ANN determines the number of targets, and the second ANN estimates their respective DOAs. The ANNs are trained using simulation data generated based on a point scatterer model in free space. The proposed approach is tested using measurement data from two loudspeakers and two walking humans in line-of-sight and through-wall environments.

1. INTRODUCTION

Through-wall human detection, tracking and imaging using radar within a highly cluttered environment is a problem of current interest [1–8]. Some potential applications include law enforcement, urban military operation, and disaster search-and-rescue. The goal is to sense humans through building walls using a radar system. For

practical use, a compact, portable device would be desirable. In this context, the use of a small sensor array is useful for finding the directions of arrival (DOAs) of humans. For example, in [7, 8] a Doppler-based sensor array with very few elements was researched to track humans, as it can offer an inexpensive way to detect moving targets in the presence of stationary clutters.

The determination of DOA using a sensor array is a well studied topic in radar [9–12]. Using a sensor array, the DOA information could be obtained by either a beam-steering method or a super-resolution algorithm. The beam-steering method attempts to find the DOA information by changing the direction of the main lobe of the array pattern and detecting the power of the received beams. The resolution in beam steering to distinguish two targets is inversely proportional to the electrical size of the array. When the available number of sensor elements is small while assuming Nyquist spatial sampling, the technique has a poor angular resolution. Nevertheless, human tracking using a four-element array was successfully demonstrated in [8]. To overcome the influence of side lobes of a strong target from overshadowing weaker targets, algorithms such as CLEAN [13] and RELAX [14] were applied. These algorithms showed promising results. However, they are computationally very expensive and can not be implemented for real-time applications. Super-resolution algorithms such as MUSIC [15] and ESPRIT [16] determine the phase angles of the arriving signals using exponential parameter estimation. They have been successfully used for high-resolution DOA estimation. However, the returns from an angularly distributed human subject may violate the data model and pose a challenge for the algorithms. The results can also be unstable when the number of sensors is small. Furthermore, correlated returns from multiple targets may further reduce their performance.

In this paper, we investigate an alternative approach for the DOA estimation of multiple humans using a small sensor array. The approach is based on an artificial neural network (ANN), which has been applied to DOA estimation problems [17–19]. Previous works used ANN to the array output with slight preprocessing for the estimation of DOA. In our approach, software beamforming is first performed on the received signals from the sensor elements. In the beamforming process, a number of overlapping beams are formed simultaneously. The received signals from all the beams produce a unique "signature" in accordance with the target locations as well as the number of targets. By properly establishing the relationship between the received signatures and the number of targets (or the target locations) via an ANN, the identification of the number of

targets (or their locations) can be carried out. In our target tracking procedure, two separate ANNs are used sequentially. The first ANN determines the number of targets, and the second ANN estimates their respective DOAs. The ANNs are trained using simulation data generated using a point scatterer model in free space. Once the ANNs are trained, they can be used to carry out the DOA estimation in real-time. The proposed approach is verified by measurements of loudspeakers and walking humans using a four-element array described in [8]. Through-wall measurements are also performed and their results are reported.

2. PROCESSING IN BEAMFORMING SPACE

2.1. Problem Formulation

Our proposed approach to estimate the number of targets and to find their DOAs can be considered as an extension of the monopulse radar concept. Monopulse is a simultaneous lobing technique for determining the angular location of a target with high resolution [20]. Two beams are generated slightly off the target direction. The ratio of the received signal strengths from the beams determines the more accurate bearing of the target. The DOA information is derived using the monopulse ratio:

$$Monopulse\ Ratio = \frac{Difference\ of\ the\ Strengths}{Sum\ of\ the\ Strengths} \qquad (1)$$

The monopulse concept improves the angular resolution, but this technique is limited to finding the DOA of a single target. When there are multiple targets, the DOA estimation may not be correct because the sidelobes of the beams can receive returns from other targets.

Here, we extend the monopulse concept by generating several beams simultaneously in order to track multiple targets using a moderate size array. In the beamforming process, a number of overlapping beams are formed. The beams are broad due to the limited size of the array. The received signal strengths from the beams form a (preferably unique) *signature* in accordance with the number of targets and their bearing locations. Therefore, by properly modeling the relationship between the signature and the number of targets (or their bearing locations), the identification of the target information may be carried out.

The signature, i.e., the relative received strengths from the different beams, plays a key role for estimating the number of targets and their DOAs. In our discussion, we normalize the signature by the total signal strength to eliminate the effects from the target range and
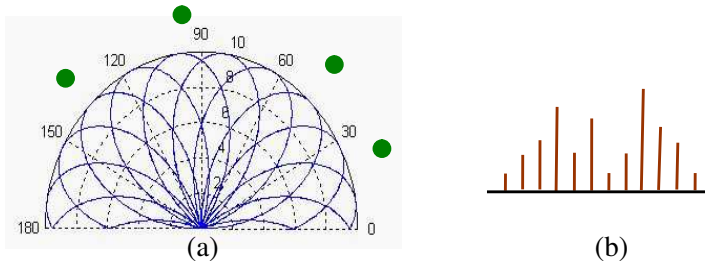
Figure 1. Multiple targets case. (a) 12 formed beams. (b) Signature consisting of the received power from all the beams.

the target radar cross section. When there is a single target, a beam directed close to the target experiences the strongest signal return. The beams directed far off the target also experience a return due to the sidelobe of its pattern. A more accurate DOA can be determined by comparing the ratio of the received strengths from adjacent beams, as is done in a monopulse radar. As the number of targets increases, the signature of the received beams becomes more complex. The received signal strength of each beam is a complex sum of returns from all the targets. Fig. 1 depicts the situation with four targets. The normalized signature is strongly related to the number of targets, their strengths, and their locations. The signature is normalized by dividing by its energy to remove the effects of distance and the RCS of the target, which are not parameters of interest in this paper.

The forward relationship can be formulated by an equation when we assume a uniform linear array. If the number of targets is N, the number of sensors is P and the number of generated beams is S, the received signal from the each beam can be expressed as

$$[E^1, E^2, \ldots, E^S] = k_1 \cdot [r_1^1, r_1^2, \ldots, r_1^S] + \ldots + k_N \cdot [r_N^1, r_N^2, \ldots, r_N^S] \quad (2)$$

where E^i is the received signal from the ith beam, k_j is the target strength of the jth target, which is a complex number, and $[r_m^1, r_m^2, \ldots, r_m^S]$ is a vector representing the phase response of the array

from the mth target represented as

$$
\begin{bmatrix} r_m^1 \\ r_m^2 \\ . \\ . \\ . \\ r_m^S \end{bmatrix} = \begin{bmatrix} \sum_{n=1}^{P} e^{-j\beta d(n-1)\sin\phi_1} \cdot e^{-j\beta d(n-1)\sin\theta_m} \\ \sum_{n=1}^{P} e^{-j\beta d(n-1)\sin\phi_2} \cdot e^{-j\beta d(n-1)\sin\theta_m} \\ . \\ . \\ . \\ \sum_{n=1}^{P} e^{-j\beta d(n-1)\sin\phi_S} \cdot e^{-j\beta d(n-1)\sin\theta_m} \end{bmatrix} \tag{3}
$$

where θ_m $(-90° < \theta_m < 90°)$ is the DOA of the mth target, ϕ_i $(-90° < \phi_i < 90°)$ is the ith beam angle, d is the antenna spacing and β $(= 2\pi/\lambda)$ is the wave number. Because each r vector is uniquely dependent on the DOA of the target, Eq. (2) can be written as:

$$
[E^1, E^2, \dots, E^S] = k_1 \cdot H(\theta_1) + \dots + k_N \cdot H(\theta_N) \tag{4}
$$

Here, the function H, which is an S-dimensional function, is assumed to be known. For a given set of E, N and θ_m are the unknown values to be estimated. The target strength k_m in Eq. (4) is dependent not only on the target range but also on the radar cross section of the target, and, is not considered of interest. While the phase information at the beam output may be informative, only the magnitude information is considered in this study. Thus, the final equation becomes:

$$
\left[\left| E^1 \right|, \dots, \left| E^S \right| \right] = abs\left(k_1 \cdot H(\theta_1) + k_2 \cdot H(\theta_2) + \dots k_N \cdot H(\theta_N) \right) \tag{5}
$$

where $abs(A)$ is the matrix where $abs(A)_i = |A_i|$. The number of targets N and the target DOAs should be determined based on the received signature $[|E^1|, \dots, |E^S|]$. Since the relationship between the signature and the information of interest is quite complex and nonlinear, we will utilize an artificial neural network to approximate the relationship.

2.2. Uniqueness of the Solution

In order to apply the ANN for DOA estimation, it should be verified that the problem is truly a regression problem, i.e., we must be able to determine a unique DOA in accordance with a given signature. If not, a high DOA estimation error will result from the ANN. In the above problem, the conditions that ensure the uniqueness of the DOA estimation are $S \geq P$ and $P \geq 2N$ ($S =$ no. of beams, $P =$ no. of sensors, $N =$ no. of targets). In this section, we prove that the solution is unique under these conditions.

The lemma we have is that the k and θ that satisfy Eq. (2) are unique for a given E when $S \geq P$ and $P \geq 2N$. If we assume that the solution is not unique so that $\langle k, \theta \rangle$ and $\langle k', \theta' \rangle$ are two sets of solutions that satisfy Eq. (2), the following equation can be written:

$$
\begin{bmatrix} E^1 \\ E^2 \\ \cdot \\ \cdot \\ E^S \end{bmatrix} = k_1 \cdot \begin{bmatrix} \sum_{n=1}^{P} e^{-j\beta d(n-1)\sin\phi_1} \cdot e^{-j\beta d(n-1)\sin\theta_1} \\ \sum_{n=1}^{P} e^{-j\beta d(n-1)\sin\phi_2} \cdot e^{-j\beta d(n-1)\sin\theta_1} \\ \cdot \\ \cdot \\ \sum_{n=1}^{P} e^{-j\beta d(n-1)\sin\phi_S} \cdot e^{-j\beta d(n-1)\sin\theta_1} \end{bmatrix} + \ldots
$$

$$
+ k_N \cdot \begin{bmatrix} \sum_{n=1}^{P} e^{-j\beta d(n-1)\sin\phi_1} \cdot e^{-j\beta d(n-1)\sin\theta_N} \\ \sum_{n=1}^{P} e^{-j\beta d(n-1)\sin\phi_2} \cdot e^{-j\beta d(n-1)\sin\theta_N} \\ \cdot \\ \cdot \\ \sum_{n=1}^{P} e^{-j\beta d(n-1)\sin\phi_S} \cdot e^{-j\beta d(n-1)\sin\theta_N} \end{bmatrix}
$$

$$
= k_1' \cdot \begin{bmatrix} \sum_{n=1}^{P} e^{-j\beta d(n-1)\sin\phi_1} \cdot e^{-j\beta d(n-1)\sin\theta_1'} \\ \sum_{n=1}^{P} e^{-j\beta d(n-1)\sin\phi_2} \cdot e^{-j\beta d(n-1)\sin\theta_1'} \\ \cdot \\ \cdot \\ \sum_{n=1}^{P} e^{-j\beta d(n-1)\sin\phi_S} \cdot e^{-j\beta d(n-1)\sin\theta_1'} \end{bmatrix} + \ldots
$$

$$
+ k_N' \cdot \begin{bmatrix} \sum_{n=1}^{P} e^{-j\beta d(n-1)\sin\phi_1} \cdot e^{-j\beta d(n-1)\sin\theta_N'} \\ \sum_{n=1}^{P} e^{-j\beta d(n-1)\sin\phi_2} \cdot e^{-j\beta d(n-1)\sin\theta_N'} \\ \cdot \\ \cdot \\ \sum_{n=1}^{P} e^{-j\beta d(n-1)\sin\phi_S} \cdot e^{-j\beta d(n-1)\sin\theta_N'} \end{bmatrix} \quad (6)
$$

If we substitute $-j\beta d$ by α, the above equation can be formatted

as:

$$(k_1 - k_1' + \ldots k_N - k_N') + (k_1 \cdot e^{\alpha \sin \theta_1} - k_1' \cdot e^{\alpha \sin \theta_1'} + \ldots$$
$$+ k_N \cdot e^{\alpha \sin \theta_N} - k_N' \cdot e^{\alpha \sin \theta_N'}) \cdot e^{\alpha \sin \phi_i} + \ldots$$
$$+ (k_1 \cdot e^{\alpha(P-1) \sin \theta_1} - k_1' \cdot e^{\alpha(P-1) \sin \theta_1'} + \ldots$$
$$+ k_N \cdot e^{\alpha(P-1) \sin \theta_N} - k_N' \cdot e^{\alpha(P-1) \sin \theta_N'}) \cdot e^{\alpha(P-1) \sin \phi_i} = 0 \qquad (7)$$

where $i = 1, 2, \ldots, S$. Eq. (7) is a $(P-1)$th order polynomial with respect to $e^{\alpha \sin \phi_i}$. From the condition of the lemma, S is equal to or greater than P.

When S is equal to P, the number of equations is same as the order of the equation. Eq. (7) can be represented in a matrix form as:

$$\begin{bmatrix} 1 & \cdots & 1 \\ e^{\alpha \sin \phi_i} & \cdots & e^{\alpha \sin \phi_S} \\ \vdots & \vdots & \vdots \\ e^{\alpha(P-1)\sin \phi_1} & \cdots & e^{\alpha(P-1)\sin \phi_S} \end{bmatrix}$$
$$\cdot \begin{bmatrix} k_1 - k_1' + \ldots k_N - k_N' \\ k_1 \cdot e^{\alpha \sin \theta_1} - k_1' \cdot e^{\alpha \sin \theta_1'} + \ldots + k_N \cdot e^{\alpha \sin \theta_N} - k_N' \cdot e^{\alpha \sin \theta_N'} \\ \vdots \\ k_1 \cdot e^{\alpha(P-1)\sin \theta_1} - k_1' \cdot e^{\alpha(P-1)\sin \theta_1'} + \ldots \\ + k_N \cdot e^{\alpha(P-1)\sin \theta_N} - k_N' \cdot e^{\alpha(P-1)\sin \theta_N'} \end{bmatrix} = 0 \qquad (8)$$

Because $\sin \phi$ is a monotonically increasing function when ϕ is from $-90 \deg$ to $90 \deg$, $e^{\alpha \sin \phi_i} \neq e^{\alpha \sin \phi_j}$ for $i \neq j$. Thus, the determinant of the left matrix, which is a Vandermonde matrix, cannot be zero, and Eq. (8) should have only a trivial solution. When S is greater than P, the number of equations is greater than the order of the equation. In this case, Eq. (7) has only a trivial solution. Therefore, the following equations should be satisfied when S is equal to or greater than P:

$$(k_1 - k_1' + \ldots k_N - k_N') = 0$$
$$(k_1 \cdot e^{\alpha \sin \theta_1} - k_1' \cdot e^{\alpha \sin \theta_1'} + \ldots + k_N \cdot e^{\alpha \sin \theta_N} - k_N' \cdot e^{\alpha \sin \theta_N'}) = 0$$
$$\cdots \qquad (9)$$
$$(k_1 \cdot e^{\alpha(P-1)\sin \theta_1} - k_1' \cdot e^{\alpha(P-1)\sin \theta_1'} + \ldots$$
$$+ k_N \cdot e^{\alpha(P-1)\sin \theta_N} - k_N' \cdot e^{\alpha(P-1)\sin \theta_N'}) = 0$$

Eq. (9) can be represented in a matrix form as:

$$A \cdot B = 0$$

where

$$A = \begin{pmatrix} 1 & -1 & \cdots & 1 & -1 \\ e^{\alpha \sin \theta_1} & -e^{\alpha \sin \theta_1'} & \cdots & e^{\alpha \sin \theta_N} & -e^{\alpha \sin \theta_N'} \\ \vdots & \vdots & \vdots & \vdots & \vdots \\ e^{\alpha \sin \theta_1 (P-1)} & -e^{\alpha \sin \theta_1' (P-1)} & \cdots & e^{\alpha \sin \theta_N (P-1)} & -e^{\alpha \sin \theta_N' (P-1)} \end{pmatrix},$$

$$B = \begin{pmatrix} k_1 \\ k_1' \\ \vdots \\ k_N \\ k_N' \end{pmatrix} \tag{10}$$

When $P \geq 2N$ from the proposition, the matrix A is not guaranteed to be a square matrix. However, A can be truncated to a $2N$ by $2N$ matrix. After truncation and moving the minus sign into k', we have the following equation:

$$\begin{pmatrix} 1 & 1 & \cdots & 1 & 1 \\ e^{\alpha \sin \theta_1} & e^{\alpha \sin \theta_1'} & \cdots & e^{\alpha \sin \theta_N} & e^{\alpha \sin \theta_N'} \\ \vdots & \vdots & \vdots & \vdots & \vdots \\ e^{\alpha \sin \theta_1 (2N-1)} & e^{\alpha \sin \theta_1' (2N-1)} & \cdots & e^{\alpha \sin \theta_N (2N-1)} & e^{\alpha \sin \theta_N' (2N-1)} \end{pmatrix}$$

$$\cdot \begin{pmatrix} k_1 \\ -k_1' \\ \vdots \\ k_N \\ -k_N' \end{pmatrix} = 0 \tag{11}$$

To obtain a non-trivial solution, the determinant of the truncated A, which is a Vandermonde matrix, must be zero:

$$\det(Truncated\ A) = 0 \tag{12}$$

Because the determinant of an n by n Vandermonde matrix is $\prod_{1 < i < j < n} (\alpha i - \alpha j)$ where αi and αj are variables of polynomials, at least two of the column vectors should be the same. For all $\theta_1 \ldots \theta_N$ and $\theta_1' \cdot \theta_N'$, Eq. (11) should be satisfied. When k and k' are all non-zero in Eq. (11):

$$e^{\alpha \sin \theta_1} = e^{\alpha \sin \theta_1'}, \ldots, e^{\alpha \sin \theta_N} = e^{\alpha \sin \theta_N'} \tag{13}$$

This can be proven through the mathematical induction. When θ is from $-90 \deg$ to $90 \deg$, $\sin \theta$ is a monotonically increasing function. Thus:

$$\theta_1 = \theta_1', \ldots, \theta_N = \theta_N'. \tag{14}$$

If we let $k_i - k_i' = Kd_i$, Eq. (11) becomes:

$$\begin{pmatrix} 1 & 1 & \cdots & 1 \\ e^{\alpha \sin \theta_1} & e^{\alpha \sin \theta_2} & \cdots & e^{\alpha \sin \theta_N} \\ \vdots & \vdots & \vdots & \vdots \\ e^{\alpha(P-1)\sin \theta_1} & e^{\alpha(P-1)\sin \theta_2} & \cdots & e^{\alpha(P-1)\sin \theta_N} \end{pmatrix} \cdot \begin{pmatrix} Kd_1 \\ Kd_2 \\ \vdots \\ Kd_N \end{pmatrix} = 0 \quad (15)$$

When $\theta_1 \neq \theta_2 \neq \ldots \neq \theta_N$, the determinant of the above Vandermonde matrix cannot be zero. Thus, Eq. (15) has only a trivial solution:

$$\begin{pmatrix} Kd_1 \\ Kd_2 \\ \vdots \\ Kd_N \end{pmatrix} = \begin{pmatrix} k_1 - k_1' \\ k_2 - k_2' \\ \vdots \\ k_N - k_N' \end{pmatrix} = 0 \quad (16)$$

From Eqs. (14) and (16), it is found that the two assumed solutions should be the same solution. Thus, the $\langle k, \theta \rangle$ that satisfies Eq. (2) is a unique solution.

To confirm the analytical result, we verify it using numerical simulations. We employ the particle swarm optimization (PSO) [21], which is a global optimizer, in a search exercise shown in Fig. 2. Given the signature E of a predefined test case, we search over all DOA values and target strength k to minimize the signature difference with the given E. The number of sensor elements is set to 4. The number of
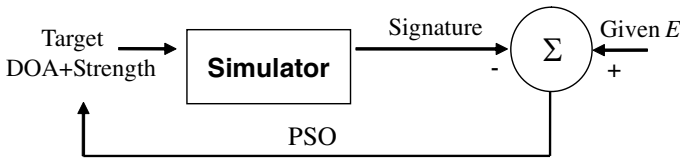

Figure 2. PSO search of DOAs and target strengths.

Table 1. The cost, DOA error and target strength error vs. different number of targets for a predefined test case.

Target Number	Cost	DOA Error (degree)	Amp. Error	Phase Error (degree)
1 Tgt	0	0	0	0
2 Tgts	1.21e-26	0	0	120.1
3 Tgts	3.23e-21	11.1	4.1	151.1
4 Tgts	8.56e-16	16.9	3.7	78.9
5 Tgts	2.34e-25	14.7	5.1	181.8

beam generated is 20. The cost function in the PSO is defined as the RMS error between the simulated signature and the given signature. After the search process, the errors in the DOA and the target strength (amplitude and phase) are tabulated. Table 1 shows the results for different number of targets.

For the single-target case, the cost, the DOA error, and target strength error are all zero. The search algorithm is able to find the correct DOA and the corresponding target strength exactly. For the two-target case, the cost is very low. The DOA error and the amplitude error are zero, leading us to conclude that the found DOA is unique and correct. Although the phase error is large, it is not relevant because only the signal strength is considered in Eq. (5). In cases with three or more targets, the DOA and target strength errors are high, even though the final cost value after the search process is very low. This implies that the search algorithm found a proper combination of DOAs and target strengths that generated almost the same signature as the given value. However, the found DOA is quite different from the actual DOA. In these cases, signature uniqueness does not hold. From this simulation, we conclude that the number of trackable targets is limited to two using a 4-element array, which is the same conclusion from the analytical solution.

3. ARTIFICIAL NEURAL NETWORK

3.1. Proposed Sequential ANN and Training Results

An ANN approach is proposed to estimate the number of targets and their DOAs based on the normalized signature at the beamformer output. An ANN is a computational model that optimizes its interconnections between artificial neurons based on external training data. After training, the ANN can describe the complex relationship between the input and output. We use a multi-layered perceptron (MLP) as our ANN structure [22].

In our problem, the number of estimated DOAs should be dependent on the number of targets. Therefore, the number of targets must first be estimated before constructing an ANN for predicting the DOA information. However, once an ANN structure is set, the number of inputs and outputs is not flexible. Therefore, we propose a sequential ANN scheme as shown in Fig. 3. The first ANN estimates the number of targets. The input to this ANN is the normalized signature. The output is the predicted number of targets. Once this first ANN is completed, a second ANN, constructed specifically for a fixed number of targets, is used to find the target DOAs. The input to the second ANN is the normalized signature and the outputs are the estimated
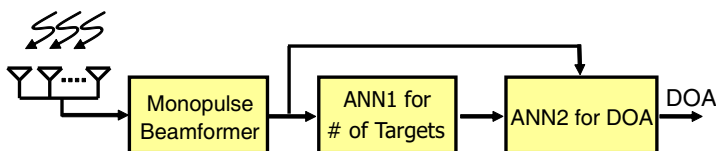
Figure 3. Proposed DOA estimation scheme.

DOAs for the specified number of targets. The number of ANNs that needs to be constructed for the second stage is the maximum possible number of targets.

To construct the ANNs, we consider a four-element linear array for illustration ($P = 4$). The normalized signatures of the received signals from many different DOAs and different number of targets are simulated for the generation of training data using Eqs. (3) and (5). A point scatterer model in free space is used for each target. In the simulation, it is assumed that the differences between target strengths ($|k|$) are less than 10 dB, and the phases ($\angle k$) are random. The number of beams formed (S) is 20. With a four-element array at half-wave spacing, the 3 dB beam width of the array is around 22 degrees. For each target, 1100 data pairs, i.e., the DOAs and their corresponding signatures, are generated by inputting random DOAs and target strengths to Eq. (5) for training and validation. If the number of targets is increased, the simulation model should be changed by adding more terms in the equation. Thus, 5500 data pairs are constructed for 5 targets ($N = 5$). To find the optimum values for the inner structure of the ANN, the training process is iterated until the validation error converges. The conjugate-gradient descent method is used in the training process. The number of hidden units is determined empirically. We increase the number of hidden units until the validation error is minimized.

First, the ANN that predicts the number of targets is trained. For the single-target case, i.e., when the training data set consists of data with only one target, 1000 data pairs are used as training data and 100 data pairs are used for validation. The resulting validation error is 0.03 (97% accuracy). When the training data set consists of data from one or two targets, 2000 data pairs are used in the training and 200 data pairs are used for validation. The resulting validation error is 0.08 (92% accuracy). As we continue to increase the number of targets, the classification errors are summarized in Table 2. From the table, it is observed that the number of targets that can be estimated with high accuracy is only two for a four-element array. For three or more targets, the validation error increases dramatically. The training time of the

Table 2. Classification error and DOA estimation error vs. number of targets.

Number of Targets	Classification Error (Accuracy)	DOA Error (degree)
1	0.03 (97%)	0.11
2	0.08 (92%)	2.42
3	0.38 (62%)	7.96
4	0.42 (58%)	13.56
5	0.54 (46%)	12.78

first ANN is 389 seconds using a Pentium dual processor (2.2 GHz) computer with 2 GB of memory. After training, the evaluation time is negligible.

The second ANN is next trained to estimate the DOAs. Depending on the number of targets, a separate ANN is constructed for each. The DOA estimation errors for different number of targets are shown in the third column of Table 1. For the single-target case, the number of output units of the ANN is one. After training, the DOA estimation error is only 0.11 degree. In the two-target case, the number of output units is two. The averaged error of the two DOAs is 2.42 degrees. However, the error increases rapidly when the number of targets is three or more. From the results, it is shown that only two targets can be tracked with high accuracy by using a four-element array. This echoes the result of the first ANN. The training time of the second ANN for two targets is 192 seconds using the same computer. After the training, the evaluation time is again negligible.

3.2. Effects of Target Strength and Number of Sensors on DOA Estimation Error

The effects of target strengths on the DOA estimation error are investigated for the two-target case for the four-sensor array. In the previous simulation, the magnitude difference of the target strengths is less than 10 dB. In order to test the effect of target strengths on the estimation error, the difference of the target strength is increased in the training data generation for the two-target case. The DOA RMS errors after training are plotted in Fig. 4. When the target strengths are exactly the same, the averaged DOA error is only 1.17 degrees. The error increases as the difference of the signal strengths is increased. This is because the influence of other targets on the signature is minor if the strength of a particular target is too strong. Beyond a 40 dB
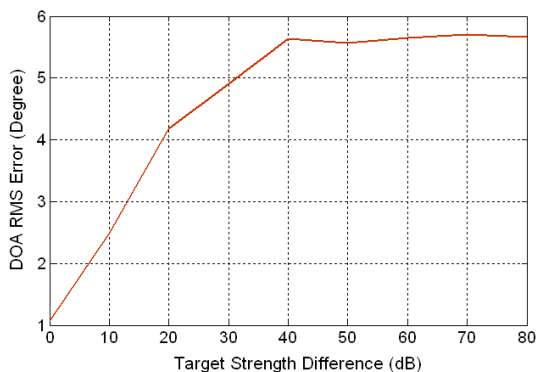
Figure 4. DOA estimation error versus difference in target strengths for the two-target case with a 4-sensor array.
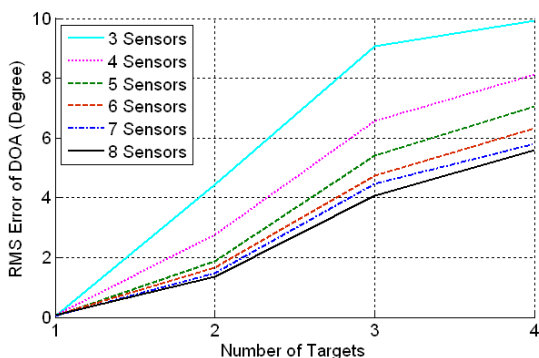

Figure 5. RMS error in DOA estimates vs. number of targets and number of sensors.

difference, the error stays around 5.7 degrees.

It is also instructive to examine the effect of the number of array elements on the DOA estimation error of multiple targets. More sensors should result in a lower estimation error. We set the difference between target strengths to be less than 10 dB and train the ANN for different numbers of sensor elements as well as for different numbers of targets. The optimal number of hidden units and the number of iterations are empirically searched for each case.

The results are presented in Fig. 5. As expected, the averaged DOA estimation error decreases as the number of sensors is increased. For the two-target case, the averaged DOA estimation error can be less than 2 degrees with five or more sensors. However, the four-

targets case results in more than 5 degrees of averaged error even with eight sensors. Thus, the proposed technique is most effective when the number of sensors and the number of targets are both small. When the number of sensors is large, other techniques such as beamforming or super-resolution algorithms may result in better performance.

4. MEASUREMENTS

4.1. Line-of-sight Measurements

Measurements of loudspeakers and humans are performed to verify the proposed method in an indoor line-of-sight environment. A receiver array that consists of four sensor elements developed previously is used to collect measurement data [8]. A horn antenna is used to transmit a continuous wave at 2.4 GHz. The transmitted power used in the measurement is 5 dBm. Four microstrip patch antennas are used as front-ends to the four receivers. The antennas are fabricated on a 1.6 mm FR-4 substrate and the element spacing is 0.56λ where $\lambda = 12.5$ cm. The gain of the individual antenna is about 0 dB. After down conversion by a quadrature mixer in each receiver, the digitized
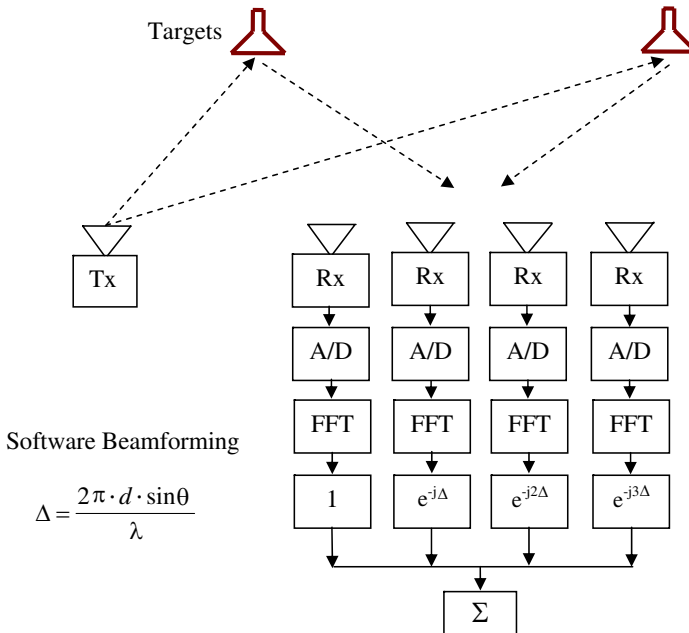

Figure 6. Experimental array configuration.

signals are stored for subsequent Doppler processing and software beamforming as shown in Fig. 6.

First, two loudspeakers are used as test targets. Both loudspeakers are driven by a 50 Hz audio signal and are located in front of the receive array. The distance between the array and the midpoint of the speakers is 3 m. The measurement setup is shown in Fig. 7. The separation between the speakers is gradually increased, resulting in a bigger angular separation between the two speakers. Before applying the proposed method, the traditional beamforming technique is first tried. The received time-domain signals from the sensors are transformed into Doppler frequency data by the fast Fourier transform (FFT). The transformed data are linearly phase-shifted and summed by software to form beams. The beam is steered by sweeping the phase shift amount. The beamforming results are presented in Fig. 8 for angular separations of 7, 14, 21 and 28 degrees. In the figure, the x axis is the angle, and the y axis is the Doppler frequency. The ± 50 Hz Doppler returns caused by the vibrating speaker membranes are clearly observed. Due to the small array aperture, the constructed beams have rather poor angular resolution. The two speakers cannot be clearly distinguished until the angular separation reaches 28 degrees in Fig. 8(d).
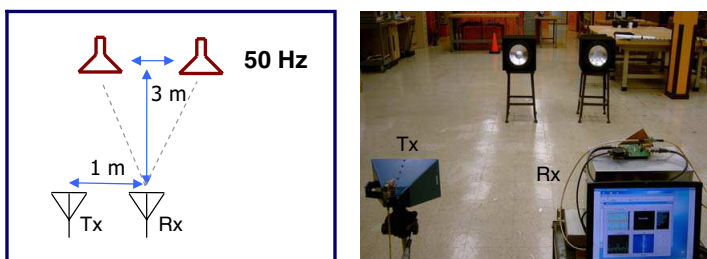

Figure 7. Measurement setup of two loudspeakers using a Doppler beamformer.

The same measured data are next processed using the proposed ANN. 20 overlapping beams are generated at 50 Hz to construct the signature, which consists of the beamformer output at a 9-degree angular sampling along the DOA axis. The signature vector is then fed as input to the trained ANN. The signatures for speaker angular separations of 7, 14, 21 and 28 degrees are shown in Fig. 9. The signatures are processed by the first ANN to estimate the number of targets. As an example, the output of the first ANN given the input signature for the 21-degree case over time is presented in Fig. 10(a). Over a two-second period, the output value of the first ANN is plotted in blue. The estimated number of targets is shown in red after rounding
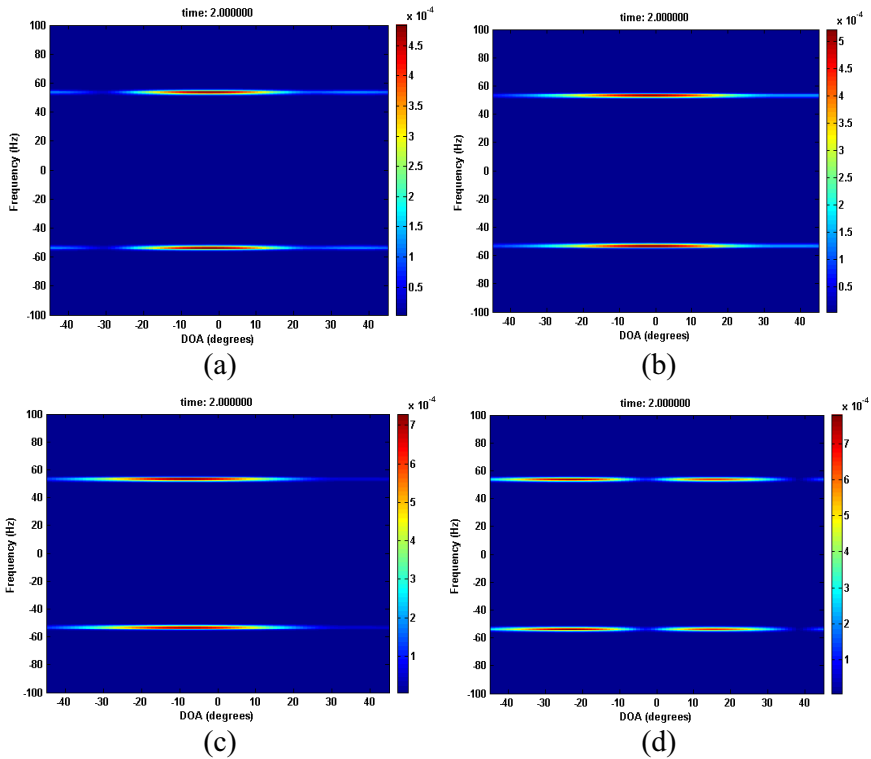
Figure 8. Beamforming results. (a) 7-degree separation. (b) 14-degree separation. (c) 21-degree separation. (d) 28-degree separation.

of the ANN output. The number of targets is correctly estimated as two.

Based on the result of the first ANN, the second ANN for the two-target case is used to determine the DOA. The outputs of the ANN are two values indicating the DOAs of the two speakers. Because the exact DOA is sensitive to the measurement setup, we instead tabulate the difference DOA of the two targets, ΔDOA. In Fig. 10(b) the estimated ΔDOA over time is depicted and compared to the actual ΔDOA. The results of the second ANN agree well with the expected ΔDOA values. The averaged ΔDOA error is about 2 degrees.

Next, two walking human subjects are measured. The heights of the two human subjects are 1.85 m and 1.76 m. The minimum distance between the humans and the radar is 3 m. One human subject walks from the left side to the right side, while the other human subject walks from the right to the left, as illustrated in Fig. 11(a). The
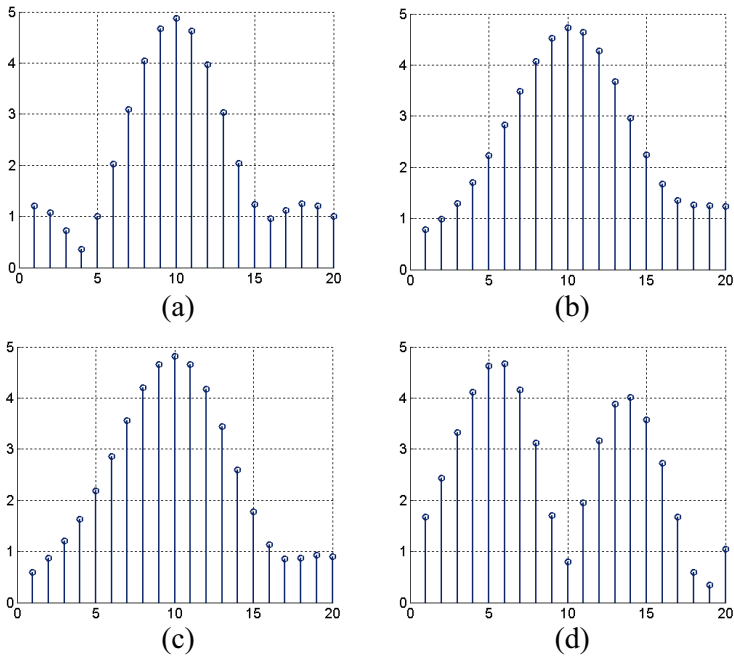
Figure 9. Sampled beamforming results. (a) 7 degree separation. (b) 14 degree separation. (c) 21 degree separation. (d) 28 degree separation.
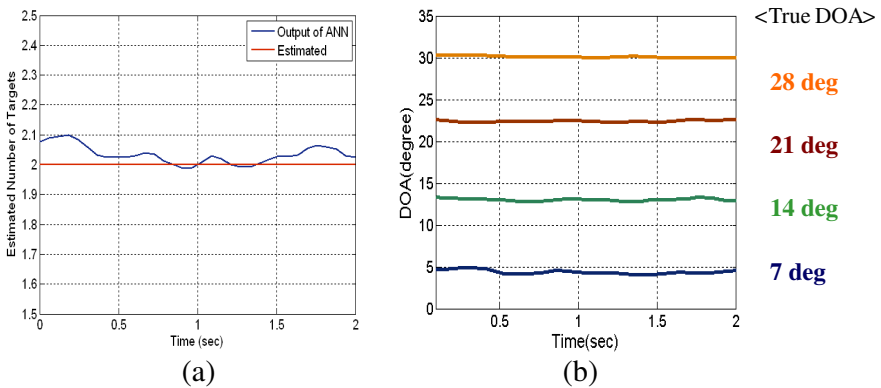

Figure 10. (a) Output of the first ANN over time. (b) Estimated ΔDOA and actual ΔDOA.

DOAs are constrained to ±45 degrees so that they do not exceed the beamwidth of the transmitting horn antenna. Fig. 11(b) shows the beamforming results for the case of the two-walking humans at a certain time instance. At this particular time instance, the two humans can be clearly observed because they have different Doppler shifts. However, when the two humans have overlapping Doppler frequencies and are close (less than 22 degrees) to each other, they become hard to discriminate using standard beamforming. In fact, because of the microDoppler spread caused by the human limbs, multiple moving humans often have significant Doppler overlap.
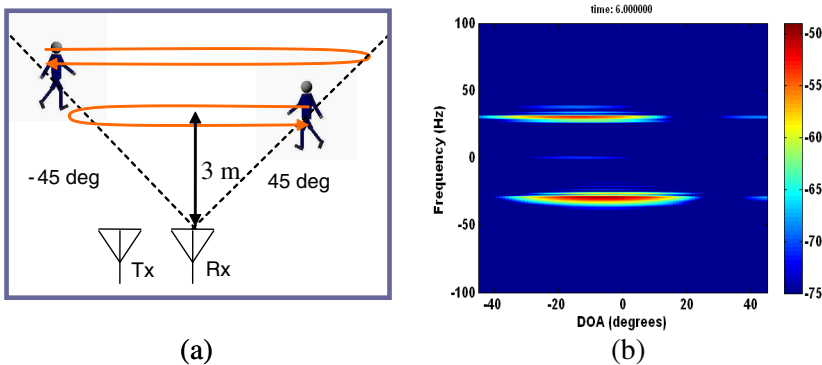

(a)   (b)

Figure 11. (a) Setup of the human tracking measurement. (b) Beamforming result from two walking humans at a certain time instance.

In our processing, we coherently sum the signal strengths along the Doppler axis in the beamforming results. By not using the Doppler separation to distinguish targets, it constitutes a more stringent test of the developed algorithm. After generating the signature, the two ANN are applied sequentially as before. The number of targets estimated using the first ANN is presented in Fig. 12(a). The output of the first ANN is plotted as a blue line. The red line is the estimated number of targets after rounding. The number of targets is correctly determined. The estimated DOA versus time using the second ANN is shown as dots in Fig. 12(b). It is observed that the DOAs of the two humans crossing each other are correctly depicted. However, the error is high when the two humans cross each other at around 7 sec. During this interval, the maximum DOA error is around 15 degrees. Outside this interval, the DOA estimation error appears to be much smaller, but the actual DOA error is difficult to compute due to the lack of ground truth DOA information. To further decrease the error requires an increase in the number of sensors, as the signature from a narrow beam can be more
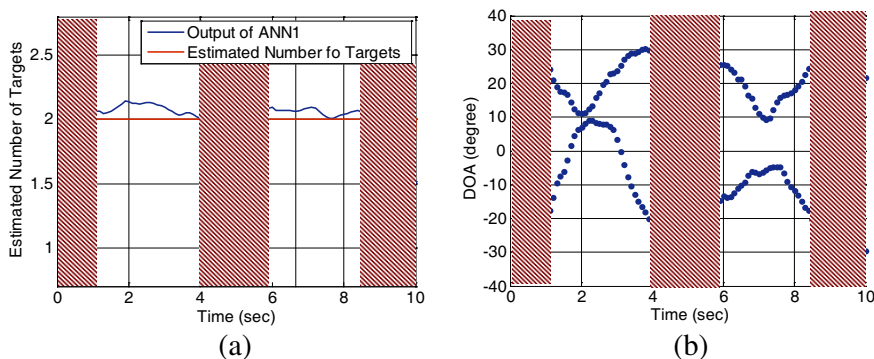
Figure 12. (a) Estimation of the number of targets from the first ANN. (b) Estimated DOAs of the two walking humans.

explicit even when two targets are close. The shaded areas are the out-of-bound regions where the DOA estimation error is high because the human subjects are beyond the beamwidth of the transmitting antenna.

4.2. Through-wall Measurements

Next, we carry out through-wall measurements and test the ANNs that were trained previously using the free-space, point-scatterer model. Of course, if the wall material is known exactly, we could in principle incorporate its property in the training process of a new set of ANNs. However, since the wall property is unknown in many practical situations, it would be instructive to see how well the simple free-space training can perform when walls are present. The two loudspeakers and two human subjects are next measured in a through-wall scenario. The transmitter and the receiver are located inside a building, and the test targets are positioned outside. The transmitted power used in the measurement is 15 dBm. The wall is a 40 cm exterior brick wall. The measurements setup is shown in Fig. 13(a). The speakers are driven with a 50 Hz audio signal again. By gradually increasing the angular separation, the estimated DOAs using the proposed method are depicted in Fig. 13(b). The actual DOAs are also noted. It is interesting to observe that the estimated DOAs are always higher than the actual DOA, possibly due to the refraction of the wall [23]. The averaged error between the estimated and the actual DOAs is 3.3 degrees, which is slightly higher than that of the line-of-sight case. Nevertheless, the ANN still seems to perform to a large extent.

Finally, two walking human subjects are measured through the
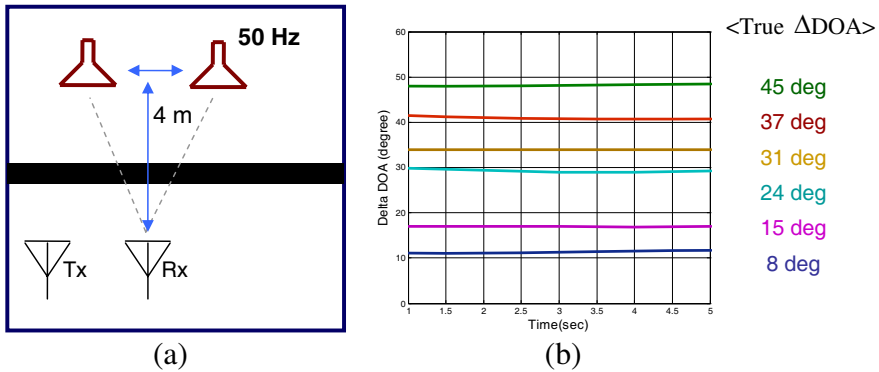
Figure 13. (a) Through-wall measurement setup. (b) Estimated DOAs from the through-wall measurement.
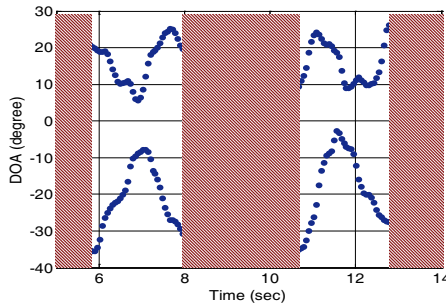

Figure 14. Estimated DOAs of the two walking humans from the through-wall measurement.

wall. The scenario is the same as the line-of-sight case. We again coherently sum the signal strengths from all the Doppler frequencies to form the signature before the DOA processing by the ANN. The DOAs of the two walking humans is presented in Fig. 14. The shaded region is when the human subjects move beyond the beamwidth of the transmitter. The overall trend of the two DOAs is correct, but the error is higher than the ling-of-sight case in Fig. 12. Also, higher error occurs when the two humans cross each other.

5. CONCLUSION

The DOAs of multiple moving humans were estimated using array processing when the number of available sensor elements is small. An extended monopulse concept was explored for the determination of

the number of targets and their DOAs based on the received signature. Two separate ANNs were constructed and used in sequence to estimate the number of targets and their DOAs. The proposed scheme was tested using measurement data from two loudspeakers and two walking humans in line-of-sight and through-wall environments. The real-time estimation method could find the DOA robust with better angular resolution as compared to the beam-steering approach.

Due to the small number of array elements, the proposed technique was found to be effective for tracking a limited number of targets. Although the number of trackable targets can be extended by increasing the number of elements, the training of the ANN can become cumbersome. In these cases, other techniques such as super-resolution algorithms may be more appropriate. In this work, we applied the ANNs trained based on the free-space assumption to measurement data from through-wall scenarios. As a result, the DOA errors were found to be higher than the errors resulting from line-of-sight data. It may be possible to reduce the error by compensating for wall refraction, provided that the wall information is known. Finally for future work, other data-driven models such as the support vector machine [24, 25] can also be tried for solving this regression problem.

ACKNOWLEDGMENT

REFERENCES

1. Frazier, L. M., "Motion detector radar for law enforcement," *IEEE Potentials*, Vol. 16, 23–26, Jan. 1998.
2. Nag, S., M. A. Barnes, T. Payment, and G. Holladay, "Ultrawideband through-wall radar for detecting the motion of people in real time," *SPIE Proc. Radar Sensor Technology and Data Visualization*, Vol. 4744, 48–57, Jul. 2002.
3. Geisheimer, J. L., E. F. Greneker, and W. S. Marshall, "High-resolution Doppler model of the human gait," *SPIE Proc. Radar Sensor Technology and Data Visualization*, Vol. 4744, 8–18, Jul. 2002.
4. Lai, C. P. and R. M. Narayanan, "Through-wall imaging and characterization of human activity using ultrawideband

(UWB) random noise radar," *Proc. of SPIE, Sensors and C3I Technologies for Homeland Security and Homeland Defense*, Vol. 5778, 186–195, May 2005.

5. Tatoian, J. Z., G. Franceshetti, H. Lackner, and G. G. Gibbs, "Through-the-wall impulse SAR experiments," *IEEE Antennas Propagat. Soc. Int. Symp.*, Jul. 2005.

6. Ahmad, F., Y. Zhang, and M. G. Amin, "Three-dimensional wideband beamforming for imaging through a single wall," *IEEE Trans. Geosci. Remote Sensing Lett.*, Vol. 5, 176–179, Apr. 2008.

7. Lin, A. and H. Ling, "A Doppler and direction-of-arrival (DDOA) radar for multiple-mover sensing based on a two-element array," *IEEE Trans. Aerosp. Electron. Syst.*, Vol. 43, 1496–1509, Oct. 2007.

8. Ram, S. S. and H. Ling, "Through-wall tracking of human movers using joint Doppler and array processing," *IEEE Trans. Geosci. Remote Sensing Lett.*, Vol. 5, 537–541, Jul. 2008.

9. Johnson, D. and D. Dudgeon, *Array Signal Processing*, Prentice Hall, 1993.

10. Trees, H. V., *Optimum Array Processing*, Wiley, 2002.

11. Liao, B., G. S. Liao, and J. Wen, "A method for DOA estimation in the presence of unknown nonuniform noise," *Journal of Electromagnetic Waves and Applications*, Vol. 22, Nos. 14–15, 2113–2123, 2008.

12. Zhang, X., X. Gao, and W. Chen, "Improved blind 2D direction of arrival estimation with L-shaped array using shift invariance property," *Journal of Electromagnetic Waves and Applications*, Vol. 23, 593–606, 2009.

13. Tsao, J. and B. D. Steinberg, "Reduction of sidelobe and speckle artifacts in microwave engineering: The CLEAN technique," *IEEE Trans. Antennas Propagation*, Vol. 36, 543–556, Apr. 1988.

14. Li, J. and P. Stoica, "Efficient mixed-spectrum estimation with applications to target feature extraction," *IEEE Trans. Signal Processing*, Vol. 44, 281–295, Feb. 1996.

15. Schmidt, R. O., "Multiple emitter location and signal parameter estimation," *IEEE Trans. Antennas Propagation*, Vol. 34, 276–280, Mar. 1986.

16. Roy, R., A. Paulraj, and T. Kailath, "ESPRIT — A subspace rotation approach to estimation of parameters of cisoids in noise," *IEEE Trans. Acoust., Speech, Signal Proc.*, Vol. 34, 1340–1342, Oct. 1986.

17. Lo, T., H. Leung, and J. Litva, "Radial basis function

neural network for direction-of-arrivals estimation," *IEEE Signal Processing Lett.*, Vol. 1, 45–47, Feb. 1994.

18. El Zooghby, A. H., C. G. Christodoulou, and M. Georgiopoulos, "A neural network-based smart antenna for multiple source tracking," *IEEE Trans. Antennas Propagation*, Vol. 48, 768–776, May 2000.

19. Vigneshwaran, S., N. Sundararajan, and P. Saratchandran, "Direction of arrival estimation under array sensor failures using a minimal resource allocation neural network," *IEEE Trans. Antennas Propagation*, Vol. 55, 334–343, 2007.

20. Sherman, S. M., *Monopulse Principles and Techniques*, Artech House, 1984.

21. Robinson, J. and Y. Rahmat-Samii, "Particle swarm optimization in electromagnetics," *IEEE Trans. Antennas Propagation*, Vol. 52, 397–407, Feb. 2004.

22. Bishop, C., *Neural Networks for Pattern Recognition*, Oxford University Press, 1995.

23. Kim, Y., "Through-wall human monitoring using data-driven models with Doppler information," Ph.D. Dissertation, The University of Texas at Austin, May 2008.

24. Kim, Y. and H. Ling, "Human activity classification based on microDoppler signatures using a support vector machine," *IEEE Trans. Geosci. Remote Sensing*, Vol. 47, 1328–1337, May 2009.

25. Bermani, E., A. Boni, A. Kerhet, and A. Massa, "Kernels evaluation of SVM-based estimators for inverse scattering problems," *Progress In Electromagnetics Research*, Vol. 53, 167–188, 2005.